tvst

Article

Retinal Oxygen Delivery and Extraction in Ophthalmologically Healthy Subjects With Different Blood Pressure Status

Konstantinos Pappelis[1,2] and Nomdo M. Jansonius[1,2]

[1] Department of Ophthalmology, University of Groningen, University Medical Center Groningen, Groningen, the Netherlands
[2] Graduate School of Medical Sciences (Research School of Behavioural and Cognitive Neurosciences), University of Groningen, Groningen, the Netherlands

Correspondence: Konstantinos Pappelis, Department of Ophthalmology, University Medical Center Groningen, P.O. Box 30.001, 9700 RB Groningen, the Netherlands. e-mail: k.pappelis@rug.nl

Received: October 1, 2021
Accepted: January 5, 2022
Published: February 4, 2022

Keywords: blood pressure; oximetry; OCT angiography; retinal blood flow; retinal metabolism

Citation: Pappelis K, Jansonius NM. Retinal oxygen delivery and extraction in ophthalmologically healthy subjects with different blood pressure status. Transl Vis Sci Technol. 2022;11(2):9, https://doi.org/10.1167/tvst.11.2.9

Purpose: To compare retinal oxygen delivery (DO_2) and oxygen extraction (VO_2) in ophthalmologically healthy subjects with different blood pressure (BP) status.

Methods: In this case-control study, we prospectively included 93 eyes of 93 subjects (aged 50–65 years) from a Dutch cohort ($n = 167{,}000$) and allocated them to four groups (low BP, normal BP [controls], treated arterial hypertension [AHT], untreated AHT). We estimated vascular calibers from fundus images and fractal dimension from optical coherence tomography angiography scans. We combined calibers, fractal dimension, BP, and intraocular pressure measurements in a proxy of retinal blood flow (RBF), using a Poiseuille-based model. We measured arterial and venous oxygen saturations (S_aO_2, S_vO_2) with a scanning laser ophthalmoscope. We calculated the DO_2 and VO_2 from the RBF, S_aO_2, and S_vO_2. We compared the DO_2 and VO_2 between groups and investigated the DO_2–VO_2 association.

Results: DO_2 and VO_2 were different between groups ($P = 0.009$, $P = 0.036$, respectively). In a post hoc analysis, the low BP group had lower DO_2 than the untreated AHT group ($P = 4.9 \times 10^{-4}$). The low BP group and the treated AHT group had a lower VO_2 than the untreated AHT group ($P = 0.021$ and $P = 0.034$, respectively). There was a significant DO_2–VO_2 correlation ($R_{obs} = 0.65$, $b_{obs} = 0.51$, $P = 2.4 \times 10^{-12}$). After correcting for shared measurement error, the slope was not significant.

Conclusions: The DO_2 and VO_2 were altered in ophthalmologically healthy subjects with different BP status. Future studies could elucidate whether these changes can explain the increased risk of ophthalmic pathologies in those subjects.

Translational Relevance: Understanding the baseline interplay between BP, retinal perfusion, and oxygenation allows for improved evaluation of retinal disease manifestation.

Introduction

Blood pressure (BP) is implicated as a risk factor in the pathogenesis of several ophthalmic diseases, including leading causes of irreversible blindness, such as glaucoma, age-related macular degeneration, and diabetic retinopathy.[1,2] Although each disease is characterized by distinct, complex pathogenetic mechanisms, the implication of blood flow and tissue oxygenation is considered to be a common denominator.[3] However, to this day, our understanding of the influence of BP on the retinal oxygenation is largely incomplete.

It has long been known that the retina is a metabolically active tissue, thus prone to reduced oxygen (O_2) supply owing to hypoperfusion.[4,5] Retinal blood flow (RBF) is mostly responsible for the O_2 supply of the inner retinal layers through the superficial and deep capillary plexus.[6] By diffusion, RBF also has a modest O_2 contribution to the photoreceptors.[7] BP is a major determinant of RBF, but, at the same time, its transient

and chronic effects are dampened by tight autoregulatory mechanisms and vascular wall remodeling, which buffer the O_2 volume delivered to the tissues (DO_2).[8–10] In addition, even when DO_2 is eventually altered, human body tissues, including the retina, are still able to control the extraction of O_2 volume (VO_2) from the circulation, up to a certain extent.[11–13] Consequently, it is difficult to a priori predict the effect of BP on retinal metabolism.

There is evidence that the concept of BP status could be more relevant to tissue oxygenation than BP alone, at least for certain ophthalmic diseases, such as glaucoma or ischemic optic neuropathy.[14–17] A low BP (especially when presented as nocturnal dipping) can directly lead to hypoperfusion, whereas a high BP can cause chronic damage to the endothelium, resulting in RBF dysregulation.[10,18] Moreover, antihypertensive treatment may or may not fully protect the tissue from ischemic damage. This factor would depend on disease stage, on the individual contribution of certain medications, or even on low BP targets.[19–22] The latter could bring the retinal vessels closer to their critical (lower) autoregulation limit, below which significant hypoperfusion may occur.[23–25]

Regardless, after the onset of any disease, it is almost impossible to disentangle the temporal relationship between perfusion deficits related to BP status and tissue apoptosis. Impaired oxygenation could simultaneously be the cause (decreased supply) and consequence (decreased demand) of cellular death. Therefore, to understand the involvement of BP in retinal disease, it is important, as a starting point, to establish how chronic BP status affects the oxygenation of the otherwise healthy retina.

The aim of this study was to compare absolute retinal O_2 delivery and extraction in ophthalmologically healthy subjects with low BP, normal BP (controls), treated arterial hypertension (AHT), and untreated AHT. For this purpose, we used previously described approaches to combine static imaging-based modeling of absolute RBF with dual-wavelength retinal oximetry.

Methods

Study Design and Population

This is a cross-sectional, case-control study. We prospectively recruited subjects participating in Lifelines Biobank, an ongoing cohort study of the northern Netherlands ($n \simeq 167{,}000$). The study comprised four groups, each one describing a distinct BP status: "low BP" (group 1), "normal BP" (group 2), that is, controls, "treated AHT" (group 3), and "untreated AHT" (group 4). The group definitions were based on information from multiple (at least two) previous visits. The exact definitions and rationale have been extensively described in our recent study on the same population.[25] In short, we required both the systolic and diastolic BP (SBP, DBP) of subjects belonging to groups 1 and 4 to consistently belong to the lowest and highest deciles of the Lifelines distribution, respectively. We also required both SBP and DBP in group 2 to fall no more than 1 standard deviation away from their means. Last, for subjects in group 3, we required uninterrupted use of antihypertensive medication for at least the past year. Invitations were sent to participants between 50 and 65 years old satisfying these BP criteria. Subjects who responded to our invitation underwent further screening for ophthalmic conditions and a general medical history interview. For each study group, the achievement of predetermined power levels (or lack of participant availability) was considered as the end of the recruitment.

We excluded participants with best-corrected visual acuity less than 0.8 (20/25), spherical refractive error larger than +3 diopters (D) or −3 D, cylinder exceeding 2 D, IOP higher than 21 mm Hg (noncontact tonometer Tonoref II, Nidek, Aichi, Japan), reproducibly abnormal visual field test locations (Frequency Doubling Technology [C20-1 screening mode], Carl Zeiss, Jena, Germany), a family history of glaucoma, and any ophthalmic pathology, including history of previous ophthalmic surgery. Absence of ophthalmic disease was confirmed with the subsequent imaging sessions (discussed elsewhere in this article). We also excluded participants with diabetes, cardiovascular disease (except for AHT in groups 3 and 4), hematologic disease, and lung disease. We did not exclude smokers, but, because early chronic obstructive pulmonary disease cannot be ruled out completely in these participants, we recorded any previous or current regular smoking.

All participants provided written informed consent. The ethics board of the University Medical Center Groningen approved the study protocol (#NL61508.042.17). The study followed the tenets of the Declaration of Helsinki.

RBF Measurements

In total, 105 participants satisfying the BP definitions and screening criteria qualified for the subsequent imaging session. Before the start of the imaging session, we performed standard on-site BP measurements. The collected imaging data relevant to this

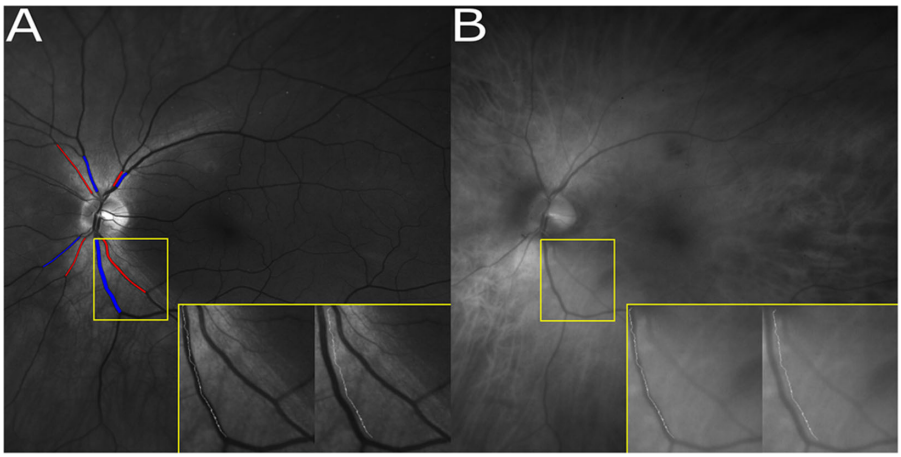

Figure 1. (A) SLO image at 532 nm. At this isosbestic ("oxygen-insensitive") wavelength, arteries and veins seem to be similar in terms of OD. Measured arterial and venous segments are marked in red and blue, respectively. The path of minimal intensity inside the vessel and a parallel path outside the vessel are shown for the IT vein. (B) SLO image at 633 nm. At this nonisosbestic ("oxygen-sensitive") wavelength, arteries appear brighter than veins, owing to higher O_2 content.

study were, in short: optic nerve head–centered fundus images, 6 × 6 mm optical coherence tomography angiography (OCTA) macula scans, and retinal images obtained with a scanning laser ophthalmoscope (SLO). The details behind fundus imaging and OCTA scans can be found in our related study on the same population, and the details behind the SLO scanning are provided elsewhere in this article.[25] For the imaging session, we selected one eye per participant. If both eyes satisfied the ophthalmic inclusion criteria, this selection was random.

RBF estimations were based on a static imaging model-based approach. This protocol has been shown to have very good agreement with in vivo RBF measurements of the human retina, assessed by Laser Speckle Flowgraphy.[24] Hereunder, we provide an outline of the procedure. After data collection, we first estimated the central retinal artery and vein equivalents, that is, vascular calibers, from fundus images and the microvascular branching complexity (fractal dimension [FD]) from en face OCTA scans, using standard methods.[26–28] In short, we used full-spectrum amplitude decorrelation angiography (Canon OCT-HS100 SD-OCT; Canon, Inc., Tokyo, Japan) to generate 6 × 6 mm images of the superficial vascular plexus, centered at the macula. We subsequently binarized the images in "flow" and "nonflow" pixels using a local Otsu thresholding algorithm.[27] The FD was ultimately calculated from the binarized images with the standard box-counting technique.[28] We then calculated total retinal vascular resistance (RVR) for each subject, by combining these measurements with blood viscosity in a Poiseuille-based fractal branching model.[24,29] Lastly, we calculated RBF from RVR and refined estimates of the retinal perfusion pressure (RPP):

$$\mathrm{RBF} = \frac{\mathrm{RPP}}{\mathrm{RVR}}, \tag{1}$$

where

$$\mathrm{RPP} = 0.39 \times \left[\mathrm{DBP} + \tfrac{1}{3}(\mathrm{SBP} - \mathrm{DBP})\right] - \mathrm{IOP} + 10.1\ \mathrm{mmHg}. \tag{2}$$

OCT and OCTA scans with an image quality of less than 7 out of 10, segmentation errors, or artifacts were excluded.[30] This resulted in the exclusion of nine subjects. All subjects had high-quality fundus images.

Oxygen Saturation Measurements

An SLO (Optomap 200Tx, Optos PLC, Dunfermline, UK) was used to measure arterial and venous O_2 saturations (S_aO_2, S_vO_2), by means of a commonly used dual-wavelength technique.[31,32] The device simultaneously acquires two retinal images, one at a wavelength of 532 nm (oxygen insensitive; Fig. 1A) and the other at a wavelength of 633 nm (oxygen sensitive; Fig. 1B). Three images per eye were obtained with the ResMax option (approximately 60°), at the same laser intensity, and with the gain set at medium iris pigmentation. Images were exported and stored in uncompressed format (.tiff). Three more subjects were excluded, owing to persistent blinking artifacts.

The optical density (OD) of a vessel at a given wavelength is defined as:

$$\mathrm{OD} = \log\left(\frac{I_{out}}{I_{in}}\right) \tag{3}$$

where I_{out} is taken equal to the average grayscale intensity over a measurement area outside the vessel and I_{in} is taken equal to the average grayscale intensity inside the vessel.

The OD ratio (ODR) of a vessel at two given wavelengths (in this case, 633 nm and 532 nm) is defined as:

$$\mathrm{ODR} = \frac{\mathrm{OD}_{633}}{\mathrm{OD}_{532}}. \quad (4)$$

By using the Beer–Lambert law, it can be shown that, under ideal conditions:

$$\mathrm{SO_2(\%)} = \frac{\alpha_{r,532} \times \mathrm{ODR} - \alpha_{r,633}}{(\alpha_{r,532} - \alpha_{o,532}) \times \mathrm{ODR} - (\alpha_{r,633} - \alpha_{o,633})} \times 100\% \quad (5)$$

where α_r is the absorption coefficient of reduced hemoglobin (Hb) and α_o is the absorption coefficient of oxyhemoglobin.

Because 532 nm is an almost isosbestic wavelength ($\alpha_{r,532} \simeq \alpha_{o,532}$) and the ODR is small, it is commonly assumed (and experimentally verified) that the SO_2 falls linearly with increasing ODR, that is:

$$\mathrm{SO_2(\%)} = (k_1 \times \mathrm{ODR} + k_2) \times 100\%, \quad (6)$$

where k_1, k_2 are constants determined after calibration.[31,33,34]

To obtain saturation values for the central retinal artery and vein, we first need to measure the saturation of their visible branches. We selected the largest artery and vein of each quadrant (superotemporal [ST], inferotemporal [IT], superonasal [SN], inferonasal [IN]) and ignored smaller vessels, because this approach has been found to minimally affect estimations.[35] To minimize O_2 diffusion losses, measurements were taken close to the border of the optic disc, according to a previously described, semiautomatic protocol.[34] In short, the path of minimal intensity (thus, avoiding the vessel light reflex) between the starting point of the vessel and the first major branching was automatically traced. A parallel path outside the vessel, at a fixed distance of 30 pixels was also traced automatically (Fig. 1). ODR was subsequently calculated, according to Equations 3 and 4, with the image grayscale value as the standard proxy for intensity.[33] For each vessel, we recorded the median of three measurements. Feasibility, repeatability, and reproducibility of this approach have been previously established, also for an SLO.[36–40]

The obtained ODR values have to be corrected for the artifactual influence of factors other than O_2 saturation, mostly related to magnification errors, heterogeneous light absorption, and photon backscattering, before they can be used to calculate SO_2 via Equation 6.[31,33,41] For each vessel segment, we implemented linear compensations by means of a backward regression model, with ODR serving as the dependent variable and the independent variables being potential confounders, that is, laterality, optic disc area, spherical error, cylinder, vessel diameter, and quadrant pigmentation index (PI). Only the significant variables of the reduced (final) model were subsequently used to construct the following correction formula:

$$\mathrm{ODR_{cor}} = \mathrm{ODR} - (b_0 + b_1X_1 + \ldots + b_nX_n) + \overline{\mathrm{ODR}}, \quad (7)$$

where ODR_{cor} is the corrected ODR, b_i are the regression coefficients, X_i are the confounders that remained in the reduced model, and $\overline{ODR}$ is the average ODR of the study population. The ODR_{cor} was evaluated for each quadrant separately.

PI was calculated based on extravascular reflection, as follows:

$$\mathrm{PI} = \log\left(\frac{I_{out,633}}{I_{out,532}}\right). \quad (8)$$

Because the increase in light absorption with increasing melanin is more pronounced at longer wavelengths, lower PI values indicate increased pigmentation.[42]

The O_2 saturation in the central retinal artery can be calculated as the average measured saturation in the four major arterial arcades:

$$S_aO_2 = \frac{S_aO_{2,ST} + S_aO_{2,IT} + S_aO_{2,SN} + S_aO_{2,IN}}{4}. \quad (9)$$

The O_2 saturation in the central retinal vein can be calculated as the average measured saturation in the four major venous arcades, weighted by the relative flow contribution of each arcade. The weight factor equals a power of the radius of the relevant venular segment[43]; the Poiseuille-based model used for absolute RBF estimations assumes that the power is equal to FD + 1.15, where FD is the two-dimensional FD measured by OCTA (see *RBF measurements*) and 1.15 is a branch length coefficient.[24,29,44] Therefore:

$$S_vO_2 = \frac{\begin{array}{l} r_{v,ST}^{FD+1.15} \times S_vO_{2,ST} + r_{v,IT}^{FD+1.15} \times S_vO_{2,IT} \\ + r_{v,SN}^{FD+1.15} \times S_vO_{2,SN} + r_{v,IN}^{FD+1.15} \times S_vO_{2,IN} \end{array}}{r_{v,ST}^{FD+1.15} + r_{v,IT}^{FD+1.15} + r_{v,SN}^{FD+1.15} + r_{v,IN}^{FD+1.15}}, \quad (10)$$

where r_v denotes the radius of the relevant venular segment.

Owing to measurement artifacts, paradoxically different arteriolar saturations may be measured in each of the four retinal quadrants. Therefore, for the sake of comparison, the weighted average calculation proposed in Equation 10 for the venules was also used for the arterioles, instead of Equation 9. Henceforth, we refer to this calculation as the "alternative S_aO_2 calculation."

Using Equations 6, 7, 9, and 10, we can express the S_aO_2 and S_vO_2 as a function of the regression coefficients b_i and the constants k_1 and k_2. As described elsewhere in this article, the b_i can be calculated from a standard linear fitting. Now, to determine k_1 and k_2, we need two distinct calibration values. The average S_aO_2 and S_vO_2 values for healthy eyes reported by Schweitzer et al.[32] (92.2% and 57.9%, respectively) are the values most frequently used for calibration. With these values, the calibration constants were $k_1 = -2.46$ and $k_2 = 1.26$. Calibration is unrestrictive and allows saturation measurements to exceed 100%, owing to variability.[37,45]

Total Retinal DO_2 and Extraction

We can now estimate the outcome variables, DO_2 and VO_2, from the Fick principle, as demonstrated by Werkmeister et al.[46]:

$$DO_2 = 1.35 \times [Hb_t] \times S_aO_2 \times RBF \quad (11)$$

$$VO_2 = 1.35 \times [Hb_t] \times (S_aO_2 - S_vO_2) \times RBF, \quad (12)$$

where $[Hb_t]$ is the total Hb concentration.

In both formulas, we omitted a term for unbound O_2 content, because it is smaller than the bound O_2 content by more than two orders of magnitude.[47] We did not obtain blood samples and we, therefore, used the average $[Hb_t]$ values reported in the Lifelines Biobank, stratified by age, sex, and BP status. For this reason, we also conducted a sensitivity analysis, repeatedly replacing the average $[Hb_t]$ values with random values taken from identical distributions. Last, the VO_2 fraction (OEF) was defined as:

$$OEF = \frac{VO_2}{DO_2} = \frac{S_aO_2 - S_vO_2}{S_aO_2}. \quad (13)$$

Statistical Analysis

We compared the general characteristics and outcome variables (DO_2 and VO_2) between the four groups, by means of analysis of variance models. Potential confounding factors from the population general characteristics were included as covariates in the outcome variable models. In a post hoc analysis, we used the Tukey honest significant differences correction to account for multiple comparisons. Whenever the analysis of variance assumptions were not met, we used Welch's analysis of variance or nonparametric tests.

To examine the overall association between the DO_2 and VO_2, we used a linear regression analysis. The observed correlation of these two variables is inflated, owing to shared measurement error, stemming from the mathematical coupling of these variables. This phenomenon is commonly reported in other systems.[13] We used the method described by Stratton et al.[48] to calculate the corrected regression coefficient. In short, we calculated a reliability coefficient r_D:

$$r_D = \frac{var(DO_2) - var(err_{DO_2})}{var(DO_2)}, \quad (14)$$

where $var(DO_2)$ denotes the variance of DO_2 and $var(err_{DO2})$ denotes the variance attributable to measurement error.

The variance attributable to measurement error, $var(err_{DO2})$, was calculated from the error variances of RBF and S_aO_2, used in the calculation of DO_2 (Eq. 11). As described by Stratton et al.,[48] these error variances need to be derived from calibration. In the absence of a gold calibration standard, the error variance of the RBF was approximated from a previous experiment in an independent population, from the residual variance of RBF fitted on in vivo Laser Speckle Flowgraphy measurements.[24] Because the physiological variation of S_aO_2 in healthy individuals is expected to be minimal, the error variance of S_aO_2 was set as equal to the observed variance of S_aO_2. The corrected slope (b_{cor}) for VO_2 as a function of DO_2 can then be calculated as:

$$b_{cor} = \frac{b_{obs} - (1 - r_D) \times b_{err}}{r_D}, \quad (15)$$

where b_{obs} is the observed slope and b_{err} the slope of measurement errors, which accounts for the covariance of the error in DO_2 and VO_2. We will not demonstrate here the detailed mathematical calculations of $var(err_{DO2})$ and b_{err}, as they are extensively provided in the aforementioned paper by Stratton et al.[48]Henceforth, all normally distributed variables are described with the mean and standard deviation. Variables with a skewed distribution are described with the median and interquartile range. All analyses were performed using R (version 3.3.3; R Foundation for Statistical Computing, Vienna, Austria) and SPSS (version 26; IBM Corp., Armonk, NY). A *P* value of 0.05 or less was considered statistically significant.

Results

General Characteristics

We excluded 12 of the 105 participants (3 from the low BP group, 3 from the control group, 4 from the treated AHT group, and 2 from the untreated AHT group), owing to artifacts or insufficient image quality

Table 1. Characteristics of the Study Population

Group Size (*N*)	Group 1 (Low BP) 30	Group 2 (Normal BP) 20	Group 3 (Treated AHT) 26	Group 4 (Untreated AHT) 17	*P* Value
Age; years [median (IQR)]	56.0 (51.0–59.3)	53.5 (51.3–60.5)	55.5 (52.8–61.0)	58.0 (53.0–61.0)	0.74
Sex, % female	93.3	50.0	42.3	47.1	**2.2×10^{-4}**
SBP, mmHg [mean (standard deviation)]	107 (9)	125 (5)	142 (18)	159 (23)	**2.1×10^{-14}**
DBP, mmHg [mean (standard deviation)]	66 (6)	79 (6)	86 (11)	99 (8)	**4.1×10^{-23}**
BMI, kg/m^2 [median (IQR)]	22.4 (21.2–24.3)	23.4 (22.2–26.7)	26.9 (24.7–29.8)	27.4 (24.3–28.5)	**5.0×10^{-6}**
Smoking, % yes	23.3	35.0	30.8	41.2	0.62
IOP, mmHg [mean (standard deviation)]	14.0 (3.0)	13.4 (3.1)	14.3 (3.0)	14.5 (3.8)	0.72
SEQ, D [mean (standard deviation)]	−0.11 (1.44)	+0.19 (1.67)	−0.23 (1.55)	−0.65 (1.58)	0.45
ONH area, mm^2 [median (IQR)]	1.89 (1.68–2.24)	1.97 (1.71–2.20)	1.94 (1.72–2.31)	1.98 (1.78–2.15)	0.81

IOP, intraocular pressure; ONH, optic nerve head; IQR, interquartile range; SEQ, spherical equivalent.

at any stage of the imaging session. This resulted in a total of 93 eyes from 93 participants being included in the analysis. Their general characteristics are summarized in Table 1. The BP measurements in this table represent the actual on-site measurements preceding the scanning; the highly significant *P* values confirm the robustness of the inclusion procedure. Groups differed furthermore significantly in sex and body mass index (BMI), which is expected owing to the prevalence of low BP in females and high BMI among hypertensives, also verified in the Lifelines cohort.[49,50] Therefore, we adjusted subsequent analyses (discussed elsewhere in this article) for sex and BMI. We additionally adjusted DO_2 and VO_2 analyses for smoking status (despite not being significantly different among groups), because it could affect the O_2 metrics.

Supplementary Table S1 displays the significant variables of the reduced linear models used for the ODR correction. Corrected ODR values per retinal quadrant and the global averages are provided in Supplementary Table S2. In general, aside from the O_2 content, the ODR values were also influenced by measurement location (quadrant), pigmentation, refractive errors, and, in some cases, eye laterality (see the Discussion).

Associations With BP Status

Table 2 summarizes the measured components used in the estimation of DO_2 and VO_2, stratified by BP status. The reported mean (standard deviation) [Hb_t] values are those of the age-matched Lifelines population. Groups were similar in terms of S_aO_2 and S_vO_2, but differed in terms of RBF, on univariable analyses. Sex, BMI, and smoking history did not confound this relationship when included as covariates, nor did they after omitting each one of the four groups from the analysis ($P >> 0.05$ in all cases). In a post hoc analysis, after adjusting for multiple comparisons, the low BP group had a significantly lower mean RBF than the untreated AHT group ($P = 0.032$).

Figure 2 shows the final outcome variables, DO_2 and VO_2, stratified by BP status. Both variables were significantly different between groups ($P = 0.009$ and $P = 0.036$, respectively) in univariable analysis and the significance of this relationship was largely unaffected when [Hb_t] values were repeatedly replaced with random values taken from the same distribution (DO_2: *P*[average] = 0.008, *P*[95% of repetitions] = 0.002–0.028; VO_2: *P*[average] = 0.025, *P*[95% of repetitions] = 0.014–0.044). The significance of this relationship was also unaffected when sex, BMI, and smoking history were included as covariates (Table 3). All three covariates had additional, independent effects, which are summarized in Table 3 (reported as coefficients from the equivalent generalized linear models). The significance of this relationship was also unaffected when the alternative S_aO_2 calculation was used inside the DO_2 and VO_2 formulas ($P = 0.005$ and $P = 0.025$, respectively). In a post hoc analysis, after adjusting for

Table 2. Group Summaries for Vascular and Oximetry Measurements

	Group 1 (Low BP)	Group 2 (Normal BP)	Group 3 (Treated AHT)	Group 4 (Untreated AHT)	*P* Value
Total RBF, µL/min [mean (standard deviation)]	40.7 (6.0)	45.7 (9.6)	45.1 (8.6)	47.6 (8.3)	**0.028**
RPP, mmHg [mean (standard deviation)]	27.2 (2.8)	33.5 (3.9)	36.6 (4.7)	41.2 (5.1)	**1.6×10^{-19}**
CRAE, µm [mean (standard deviation)]	172 (12)	162 (12)	154 (13)	148 (7)	**7.0×10^{-10}**
CRVE, µm [mean (standard deviation)]	228 (18)	229 (16)	229 (18)	223 (12)	0.57
OCTA FD [mean (standard deviation)]	1.625 (0.005)	1.626 (0.007)	1.624 (0.006)	1.626 (0.006)	0.67
[Hb_t]*, g/dL [mean (standard deviation)] (population-based data)	13.6 (0.8)	14.3 (0.8)	14.2 (0.9)	14.7 (0.8)	**5.3×10^{-307}**
S_aO_2 (%) [mean (standard deviation)]	94.7 (12.8)	88.6 (12.4)	89.3 (11.2)	96.3 (12.7)	0.12
S_aO_2 (%) [mean (standard deviation)] (alternative calculation)	91.5 (11.7)	87.7 (12.3)	87.5 (12.4)	94.2 (11.8)	0.22
S_vO_2 (%) [mean (standard deviation)]	59.1 (14.2)	53.2 (13.6)	60.2 (14.5)	56.3 (14.8)	0.36

CRAE, central retinal artery equivalent; CRVE, central retinal vein equivalent.
*Data and comparison taken from Lifelines ($n = 28{,}888$).

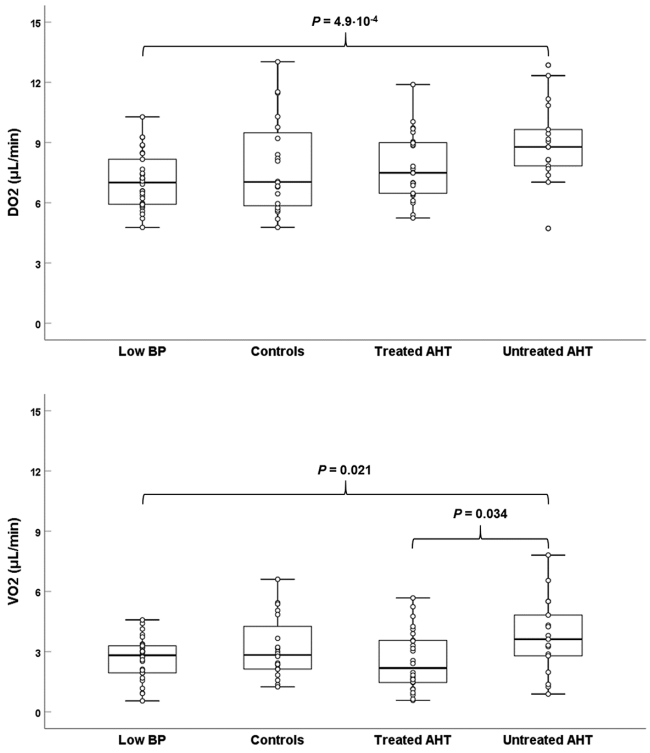

Figure 2. Total retinal DO_2 and extraction (VO_2) as a function of BP status. DO_2 is higher in subjects with untreated AHT, compared with the low BP group. The VO_2 is higher in subjects with untreated AHT, compared with both the low BP and the treated AHT group.

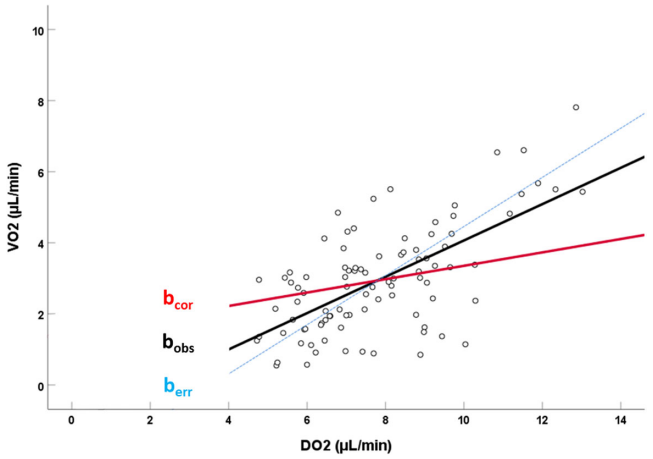

Figure 3. Pooled ($n = 93$) data for total retinal VO_2 plotted as a function of total retinal DO_2. The observed slope of the linear relationship (*continuous black line*) is denoted by b_{obs}. The component of the slope (*dashed blue line*) introduced purely via shared measurement error, owing to mathematical coupling of the two variables, is denoted by b_{err}. The true, corrected slope of the relationship (continuous red line), that is, adjusted for shared measurement error, is denoted by b_{cor}. The small, nonsignificant slope of the true relationship indicates little interdependency of resting DO_2 and VO_2.

multiple comparisons, the low BP group had a significantly lower estimated marginal mean DO_2 than the untreated AHT group ($P = 4.9 \times 10^{-4}$), whereas both the low BP group and the treated AHT group had a significantly lower estimated marginal mean VO_2 than the untreated AHT group ($P = 0.021$ and $P = 0.034$, respectively).

The mean (standard deviation) OEF was 0.37 (0.15) and was similar between groups ($P = 0.20$). In multivariable analysis, smoking was associated with a decrease in the OEF ($b = -0.07$, $P = 0.039$).

DO_2–VO_2 Relationship

The pooled ($n = 93$) association of DO_2 and VO_2 is plotted in Figure 3. Initially, there was a significant positive correlation between the two variables ($R_{obs} = 0.65$, $b_{obs} = 0.51$, $P = 2.4 \times 10^{-12}$; $R_{obs} = 0.64$, $b_{obs} = 0.50$, $P = 8.1 \times 10^{-12}$ with the alternative S_aO_2 calculation). However, after correcting for shared measurement error owing to mathematical coupling, the true slope was flatter and no longer statistically significant ($b_{cor} = 0.19$, $P = 0.29$), and the true correlation coefficient could not be calculated.[48]

Table 3. Factors Associated With DO_2 and VO_2 in Multivariable Analysis

	DO_2 (µL/min)		VO_2 (µL/min)	
	Coefficient	*P* Value	Coefficient	*P* Value
BP status; ref.: untreated AHT				
Low BP	−2.4	**2.2×10^{-5}**	−1.4	**0.002**
Normal BP	−1.5	0.013	−0.9	0.042
Treated AHT	−1.1	0.041	−1.2	**0.003**
BMI; kg/m^2	−0.14	**0.027**	−0.13	**0.006**
Sex; female = 1	NS	NS	−0.7	**0.038**
Smoking; yes = 1	NS	NS	−0.7	**0.017**

NS, not significant.
For the BP status, $P = 0.008$ is taken as the adjusted threshold of significance.

Discussion

In this study, we showed that BP status was associated with altered total retinal DO_2 and extraction (VO_2) at rest in ophthalmologically healthy subjects. Specifically, we reported an increase in the DO_2 and VO_2 with increasing BP, which was more prominent at the tails of the BP distribution. In addition, the VO_2 was also higher in subjects with untreated AHT than in subjects with treated AHT. The true association between the DO_2 and VO_2 was, at best, weak, suggesting these variables are mostly independent at rest.

Oxygen Delivery

Although the average RPP increased by 51% on the way from the low BP group to the untreated hypertensives (Table 3), the average RBF only increased by 17% (Table 3) and the average DO_2 by 27% (Table 3, Fig. 2). As a result, the differences in the RBF and DO_2 were noted as significant only between the groups representing the tails of the BP distribution. This observation is not surprising, and it is consistent with the general concept of RBF autoregulation and with the subsequent structural remodeling of blood vessels, after chronic BP elevation.[8,10,51] Experimental studies and mathematical models have shown an increase in the tissue oxygen partial pressure with transient BP manipulations.[52,53] Our results suggest that chronic low or high, but still physiological, resting BP values can also have a subtle effect on the DO_2. The increase in the DO_2 (which is the product of the RBF and O_2 content) with increasing BP was larger than that of the RBF alone. Because the S_aO_2 was similar between the groups (Table 3), this is mostly owing to the increasing [Hb_t] with increasing BP (Table 3). This association is known from other population studies.[54,55]

A higher BMI was found to be independently associated with a reduced DO_2, but not RBF, which likely reflects the documented effects of obesity on lung function and pulmonary gas exchange.[56]

Oxygen Extraction

A significantly higher VO_2 was also observed in untreated hypertensives (Table 3, Fig. 2), relative to subjects with a low BP (+41%) and treated hypertensives (+46%). Again, no group was significantly different from controls, after adjusting for multiple comparisons (Table 3). The smaller effect size, in combination with the high variability that is present in our estimates, seems to be the most likely explanation for this phenomenon. Indeed, although our average estimates for both DO_2 and VO_2 are similar to previously published values (and almost identical when the same calibration values are used), the variability we report is higher.[46,47] This outcome was owing to the larger error introduced by the SLO-based retinal oximetry (which is consistently present in all studies using the SLO), compared with the error yielded by tailored fundus cameras.[37,39,40]

The reported alterations in the VO_2 can have a number of pathophysiological explanations. We have recently shown that, in the same population, the low BP group and the treated hypertensives were characterized by a subtle thinning of the ganglion cell–inner plexiform layer and the macular and peripapillary retinal nerve fiber layer.[25] Although we do not know for sure if these insults are primary or secondary to a decreased DO_2, a lower VO_2 in these groups could, at least partially, suggest a current state of decreased O_2 demand. However, a thinning of the inner retina was also present (albeit less pronounced) in the untreated hypertensive group, which contradicts the higher average VO_2 reported for these subjects. In this regard, in the next paragraphs we speculate about the potential mechanisms that could explain this finding.

First, it is estimated that about 15% of the O_2 extracted from the retinal circulation is not consumed by the inner retina, but actually complements the choroidal O_2 supply of the photoreceptors in the outer retina. As a result, any condition that compromises the choroidal supply could lead to a compensatory increase in the retinal VO_2.[7] This VO_2 increase has already been observed in mice with early diabetes, although it has also been reported that deficits in the deep retinal capillary plexus in human diabetics are associated with photoreceptor loss.[57,58] This could also apply to AHT, because it has been shown that AHT, especially when poorly controlled, has a detrimental effect on the choriocapillaris.[59] The magnitude of this effect is unknown, but it should be able to counteract opposing forces that would tend to decrease the VO_2, at least theoretically, such as a decreased mean circulation time, shunting of flow, and deep capillary rarefaction.[60,61]

Second, experimental evidence and mathematical models support that, in the presence of increased O_2 availability, the O_2 consumption of the inner retina (especially that of the inner and outer plexiform layers) increases, a mechanism that helps to keep the inner retinal O_2 levels relatively stable.[6,52,62,63] This could pertain to subjects with untreated, chronic AHT. Indeed, although hyperoxic conditions such as 100% oxygen breathing achieve control O_2 levels mostly by inducing RBF reduction through vasoconstriction, this is obviously not possible in conditions where RBF is a priori increased, despite vessels being already

constricted.[64] Increased resting consumption in these subjects could, at least partially, explain an increased VO_2.

That said, the true correlation analysis for DO_2–VO_2 indicates that this increase in resting O_2 consumption with increased resting delivery cannot be too pronounced, if any. Indeed, although mitochondrial oxidative phosphorylation could act as a sensor of O_2 tension, it also has a saturation ceiling.[65] It is not impossible, nevertheless, that a metabolic transition to a more oxidative state, with decreased glycolytic activity, occurs.[66] Other factors could also play a role in determining the DO_2–VO_2 slope. With constant consumption, an increase in the BP would initially cause an increase in RBF (and DO_2), which would be compensated by autoregulation. Now, with constant BP, an increase in consumption would cause an increase in local CO_2, inducing vasodilation, thus causing an increase in DO_2. The gain of this feedback loop at equilibrium is possibly a major determinant of this slope and is, therefore, likely close to zero.

A higher BMI was, again, independently associated with a decreased VO_2, possibly pointing toward a decreased retinal function owing to oxidative stress and inflammation.[67] The VO_2 was lower in females than males, on which conflicting evidence exists, and could reflect the lower systemic basal metabolic rate.[47,68] Smoking was also associated with a decreased VO_2 and could be related to the reported decreased O_2 uptake present in other systems. Last, although the average, resting OEF was consistent with previous reports, we found that it was lower in smokers.[11] Studies with a tailored design could shed more light on these secondary observations.

Study Strengths and Limitations

To our knowledge, this study is the first to describe alterations in the DO_2 and VO_2 with different chronic BP status. The strict selection process that we implemented within the setting of a large-scale cohort (Lifelines Biobank) enabled us to investigate the true tails of the BP distribution. Another novelty of our study is the fact that we describe the true resting DO_2–VO_2 relationship in the retina, which avoids overestimations originating from mathematical coupling. However, there are several limitations that should be considered.

First, the calculation of the outcome variables (DO_2 and VO_2) is liable to the propagation of error associated with their measured components. Similar to other systems, the retinal DO_2 and VO_2 are not directly measured, but estimated from the multiplication of RBF with oxygen saturation (Equations 12 and 13). There is currently no gold standard way to measure these components in the clinic and there remain unresolved technical considerations with regard to acquisition and quantification. As such, any in vivo validation of these estimates remains liable itself to the same mathematical approximations. We only expect a small contribution of RBF measurements to this error for two reasons: first, RBF estimations are in very good agreement with Doppler OCT studies and, second, we have previously shown that RBF estimations strongly correlate with in vivo blood flow metrics across a large BP range, as assessed by Laser Speckle Flowgraphy on an independent validation dataset.[24,46,69–73] However, elsewhere in this article, we discussed how the more substantial error introduced by variability in oximetry measurements could have affected certain results. A lot of this variability is likely of a technical nature, owing to the documented presence of unaccounted nonuniform magnification, distortion, and illumination in particular parts of the retinal image, which can affect measurements, even with changes in the angle of gaze.[38,74] These observations can explain the unexpected between-eye ODR differences that were present in certain retinal quadrants (Supplementary Table S1). Device-specific preprocessing of the SLO images and suboptimal wavelengths are likely other sources of this increased variability. Of course, physiological effects could also result in additional optical artifacts.[75] That said, owing to the incorporation of this expected variability to our original power analysis, our study was still able to show significant effects, despite the noise introduced by measurement uncertainty.

Second, this cross-sectional study cannot conclude if and how these initial BP-related alterations in O_2 transport pertain to the development of ophthalmic pathologies. Owing to the cross-sectional nature of the study, we also did not have robust information regarding the onset and duration of AHT. However, the incorporation of BP measurements from multiple previous occasions in the group definitions, as well as the requirement of uninterrupted use of antihypertensive medication over (at least) the past year resulted in almost all diagnoses occurring before at least three years.

Last, this population was almost entirely Caucasian and, as such, any results derived from it should not be immediately generalized to other ethnicities.

Implications and Conclusions

By showing that BP-related alterations in O_2 transport may already exist in subjects with no signs of

ophthalmic pathology, this study enhances our understanding of the baseline interplay between BP, RBF, and retinal oxygenation. This finding is important, but is merely a first step toward answering pertinent questions regarding the disease process. If hypoxia plays a role in complicated pathologies such as age-related macular degeneration and diabetic retinopathy, when does the retina really become hypoxic and how early can we detect it in clinical practice?[7] Can we use this information to evaluate treatments and slow disease progression? A special mention should be made at this point for glaucoma: according to the "chicken–egg" dilemma, structural loss could be both cause and consequence of impaired blood flow.[76] In this regard, future studies could examine whether deficits in perfusion and oxygenation related to known glaucoma risk factors, such as BP status, can be helpful in stratifying the risk of incidence and/or progression of the disease.

In conclusion, we reported alterations in retinal DO_2 and VO_2 in ophthalmologically healthy subjects with different BP status. Future studies should incorporate the vascular supply of the choroid to elucidate whether increased VO_2 in uncontrolled AHT could be the result of compensatory mechanisms in effect. Longitudinal studies could investigate whether compromised delivery and extraction in subjects with low BP and treated AHT can explain the increased risk of glaucomatous damage in these population groups.

Acknowledgments

Supported by European Union's Horizon 2020 Innovative Training Networks Program, under the Marie Sklodowska – Curie grant, Project ID 675033. The funding organization had no role in the design, conduct, analysis, or publication of this research.

Meeting presentation: European Association for Vision and Eye Research (EVER); Nice, 3rd–6th October 2018.

Disclosure: **K. Pappelis**, None; **N.M. Jansonius**, None

References

1. GBD 2019 Blindness and Vision Impairment Collaborators, Vision Loss Expert Group of the Global Burden of Disease Study. Causes of blindness and vision impairment in 2020 and trends over 30 years, and prevalence of avoidable blindness in relation to VISION 2020: the Right to Sight: an analysis for the Global Burden of Disease Study. *Lancet Glob Health*. 2021;9(2):e144–e160.
2. Wong TY, Mitchell P. The eye in hypertension. *Lancet*. 2007;369:425–435.
3. Kur J, Newman EA, Chan-Ling T. Cellular and physiological mechanisms underlying blood flow regulation in the retina and choroid in health and disease. *Prog Retin Eye Res*. 2012;31:377–406.
4. Anderson B, Jr, Saltzman HA. Retinal oxygen utilization measured by hyperbaric blackout. *Arch Ophthalmol*. 1964;72:792–795.
5. Anderson B, Jr. Ocular effects of changes in oxygen and carbon dioxide tension. *Trans Am Ophthalmol Soc*. 1968;66:423–474.
6. Yu DY, Cringle SJ. Oxygen distribution and consumption within the retina in vascularised and avascular retinas and in animal models of retinal disease. *Prog Retin Eye Res*. 2001;20:175–208.
7. Linsenmeier RA, Zhang HF. Retinal oxygen: from animals to humans. *Prog Retin Eye Res*. 2017;58:115–151.
8. Riva CE, Grunwald JE, Petrig BL. Autoregulation of human retinal blood flow. An investigation with laser Doppler velocimetry. *Invest Ophthalmol Vis Sci*. 1986;27:1706–1712.
9. Pournaras CJ, Rungger-Brändle E, Riva CE, Hardarson SH, Stefansson E. Regulation of retinal blood flow in health and disease. *Prog Retin Eye Res*. 2008;27:284–330.
10. Lehmann MV, Schmieder RE. Remodeling of retinal small arteries in hypertension. *Am J Hypertens*. 2011;24:1267–1273.
11. Felder AE, Wanek J, Blair NP, Shahidi M. Inner retinal oxygen extraction fraction in response to light flicker stimulation in humans. *Invest Ophthalmol Vis Sci*. 2015;56:6633–6637.
12. Palkovits S, Told R, Schmidl D, et al. Regulation of retinal oxygen metabolism in humans during graded hypoxia. *Am J Physiol Heart Circ Physiol*. 2014;307:H1412–H1418.
13. Vincent J-L, De Backer D. Oxygen transport-the oxygen delivery controversy. *Intensive Care Med*. 2004;30:1990–1996.
14. Topouzis F, Wilson MR, Harris A, et al. Association of open-angle glaucoma with perfusion pressure status in the Thessaloniki Eye Study. *Am J Ophthalmol*. 2013;155:843–851.
15. Leeman M, Kestelyn P. Glaucoma, blood pressure. *Hypertension*. 2019;73:944–950.
16. Hayreh SS, Podhajsky P, Zimmerman MB. Role of nocturnal arterial hypotension in optic nerve head ischemic disorders. *Ophthalmologica*. 1999;213:76–96.

17. Memarzadeh F, Ying-Lai M, Chung J, Azen SP, Varma R, Los Angeles Latino Eye Study Group. Blood pressure, perfusion pressure, and open-angle glaucoma: the Los Angeles Latino Eye Study. *Invest Ophthalmol Vis Sci*. 2010;51:2872–2877.
18. Bowe A, Grünig M, Schubert J, et al. Circadian variation in arterial blood pressure and glaucomatous optic neuropathy—a systematic review and meta-analysis. *Am J Hypertens*. 2015;28(9):1077–1082.
19. Zheng W, Dryja TP, Wei Z, et al. Systemic medication associations with presumed advanced or uncontrolled primary open-angle glaucoma. *Ophthalmology*. 2018;125:984–993.
20. Chong RS, Chee M-L, Tham Y-C, et al. Association of antihypertensive medication with retinal nerve fiber layer and ganglion cell-inner plexiform layer thickness. *Ophthalmology*. 2021;128:393–400.
21. Pappelis K, Loiselle AR, Visser S, Jansonius NM. Association of systemic medication exposure with glaucoma progression and glaucoma suspect conversion in the Groningen Longitudinal Glaucoma Study. *Invest Ophthalmol Vis Sci*. 2019;60:4548–4555.
22. Horwitz A, Klemp M, Jeppesen J, Tsai JC, Torp-Pedersen C, Kolko M. Antihypertensive medication postpones the onset of glaucoma: evidence from a nationwide study. *Hypertension*. 2017;69:202–210.
23. He Z, Vingrys AJ, Armitage JA, Bui BV. The role of blood pressure in glaucoma. *Clin Exp Optom*. 2011;94:133–149.
24. Pappelis K, Choritz L, Jansonius NM. Microcirculatory model predicts blood flow and autoregulation range in the human retina: in vivo investigation with laser speckle flowgraphy. *Am J Physiol Heart Circ Physiol*. 2020;319:H1253–H1273.
25. Pappelis K, Jansonius NM. U-shaped effect of blood pressure on structural OCT metrics and retinal perfusion in ophthalmologically healthy subjects. *Invest Ophthalmol Vis Sci*. 2021;62:5.
26. Knudtson MD, Lee KE, Hubbard LD, Wong TY, Klein R, Klein BEK. Revised formulas for summarizing retinal vessel diameters. *Curr Eye Res*. 2003;27:143–149.
27. Pappelis K, Jansonius NM. Quantification and repeatability of vessel density and flux as assessed by optical coherence tomography angiography. *Transl Vis Sci Technol*. 2019;8:3.
28. Al-Nosairy KO, Prabhakaran GT, Pappelis K, Thieme H, Hoffmann MB. Combined multi-modal assessment of glaucomatous damage with electroretinography and optical coherence tomography/angiography. *Transl Vis Sci Technol*. 2020;9:7.
29. Takahashi T, Nagaoka T, Yanagida H, et al. A mathematical model for the distribution of hemodynamic parameters in the human retinal microvascular network. *J Biorheol*. 2009;23:77–86.
30. Spaide RF, Fujimoto JG, Waheed NK. Image artifacts in optical coherence tomography angiography. *Retina*. 2015;35:2163–2180.
31. Beach JM, Schwenzer KJ, Srinivas S, Kim D, Tiedeman JS. Oximetry of retinal vessels by dual-wavelength imaging: calibration and influence of pigmentation. *J Appl Physiol*. 1999;86:748–758.
32. Schweitzer D, Hammer M, Kraft J, Thamm E, Königsdörffer E, Strobel J. In vivo measurement of the oxygen saturation of retinal vessels in healthy volunteers. *IEEE Trans Biomed Eng*. 1999;46:1454–1465.
33. Hammer M, Vilser W, Riemer T, Schweitzer D. Retinal vessel oximetry-calibration, compensation for vessel diameter and fundus pigmentation, and reproducibility. *J Biomed Opt*. 2008;13:054015.
34. Geirsdottir A, Palsson O, Hardarson SH, Olafsdottir OB, Kristjansdottir JV, Stefánsson E. Retinal vessel oxygen saturation in healthy individuals. *Invest Ophthalmol Vis Sci*. 2012;53:5433–5442.
35. Heitmar R, Cubbidge RP. Retinal vessel oxygen saturation measurement protocols and their agreement. *Transl Vis Sci Technol*. 2020;9:17.
36. Yip W, Siantar R, Perera SA, et al. Reliability and determinants of retinal vessel oximetry measurements in healthy eyes. *Invest Ophthalmol Vis Sci*. 2014;55:7104–7110.
37. Kristjansdottir JV, Hardarson SH, Halldorsson GH, Karlsson RA, Eliasdottir TS, Stefánsson E. Retinal oximetry with a scanning laser ophthalmoscope. *Invest Ophthalmol Vis Sci*. 2014;55:3120–3126.
38. Palsson O, Geirsdottir A, Hardarson SH, Olafsdottir OB, Kristjansdottir JV, Stefánsson E. Retinal oximetry images must be standardized: a methodological analysis. *Invest Ophthalmol Vis Sci*. 2012;53:1729–1733.
39. Blair NP, Wanek J, Felder AE, et al. Retinal oximetry and vessel diameter measurements with a commercially available scanning laser ophthalmoscope in diabetic retinopathy. *Invest Ophthalmol Vis Sci*. 2017;58:5556–5563.
40. Vehmeijer WB, Magnusdottir V, Eliasdottir TS, Hardarson SH, Schalij-Delfos NE, Stefánsson E. Retinal oximetry with scanning laser ophthalmoscope in infants. *PLoS One*. 2016;11:e0148077.

41. Lim LS, Lim XH, Tan L. Retinal vascular oxygen saturation and its variation with refractive error and axial length. *Transl Vis Sci Technol*. 2019;8:22.
42. Delori FC, Pflibsen KP. Spectral reflectance of the human ocular fundus. *Appl Opt*. 1989;28:1061–1077.
43. Aschinger GC, Schmetterer L, Fondi K, Aranha Dos et al. Effect of diffuse luminance flicker light stimulation on total retinal blood flow assessed with dual-beam bidirectional Doppler OCT. *Invest Ophthalmol Vis Sci*. 2017;58:1167–1178.
44. Kamiya A, Takahashi T. Quantitative assessments of morphological and functional properties of biological trees based on their fractal nature. *J Appl Physiol*. 2007;102:2315–2323.
45. Garg AK, Knight D, Lando L, Chao DL. Advances in retinal oximetry. *Transl Vis Sci Technol*. 2021;10(2):5.
46. Werkmeister RM, Schmidl D, Aschinger G, et al. Retinal oxygen extraction in humans. *Sci Rep*. 2015;5:15763.
47. Bata AM, Fondi K, Szegedi S, et al. Age-related decline of retinal oxygen extraction in healthy subjects. *Invest Ophthalmol Vis Sci*. 2019;60:3162–3169.
48. Stratton HH, Feustel PJ, Newell JC. Regression of calculated variables in the presence of shared measurement error. *J Appl Physiol*. 1987;62:2083–2093.
49. Tigchelaar EF, Zhernakova A, Dekens JAM, et al. Cohort profile: LifeLines DEEP, a prospective, general population cohort study in the northern Netherlands: study design and baseline characteristics. *BMJ Open*. 2015;5:e006772.
50. Slagter SN, van Waateringe RP, van Beek AP, van der Klauw MM, Wolffenbuttel BHR, van Vliet-Ostaptchouk JV. Sex, BMI and age differences in metabolic syndrome: the Dutch Lifelines Cohort Study. *Endocr Connect*. 2017;6:278–288.
51. Tani T, Nagaoka T, Nakabayashi S, Yoshioka T, Yoshida A. Autoregulation of retinal blood flow in response to decreased ocular perfusion pressure in cats: comparison of the effects of increased intraocular pressure and systemic hypotension. *Invest Ophthalmol Vis Sci*. 2014;55:360–367.
52. Yu DY, Cringle SJ, Alder VA, Su EN. Intraretinal oxygen distribution in rats as a function of systemic blood pressure. *Am J Physiol*. 1994;267:H2498–H2507.
53. Causin P, Guidoboni G, Malgaroli F, Sacco R, Harris A. Blood flow mechanics and oxygen transport and delivery in the retinal microcirculation: multiscale mathematical modeling and numerical simulation. *Biomech Model Mechanobiol*. 2016;15:525–542.
54. Atsma F, Veldhuizen I, de Kort W, van Kraaij M, Jong PP, Deinum J. Hemoglobin level is positively associated with blood pressure in a large cohort of healthy individuals. *Hypertension*. 2012;60(4):936–941.
55. Cirillo M, Laurenzi M, Trevisan M, Stamler J. Hematocrit, blood pressure, and hypertension. The Gubbio Population Study. *Hypertension*. 1992;20:319–326.
56. Kapur VK, Wilsdon AG, Au D, et al. Obesity is associated with a lower resting oxygen saturation in the ambulatory elderly: results from the cardiovascular health study. *Respir Care*. 2013;58:831–837.
57. Liu W, Wang S, Soetikno B, et al. Increased retinal oxygen metabolism precedes microvascular alterations in type 1 diabetic mice. *Invest Ophthalmol Vis Sci*. 2017;58:981–989.
58. Scarinci F, Jampol LM, Linsenmeier RA, Fawzi AA. Association of diabetic macular nonperfusion with outer retinal disruption on optical coherence tomography. *JAMA Ophthalmol*. 2015;133:1036–1044.
59. Chua J, Le T-T, Tan B, et al. Choriocapillaris microvasculature dysfunction in systemic hypertension. *Sci Rep*. 2021;11:4603.
60. Leskova W, Warar R, Harris NR. Altered retinal hemodynamics and mean circulation time in spontaneously hypertensive rats. *Invest Ophthalmol Vis Sci.* 2020;61:12.
61. Chua J, Chin CWL, Hong J, et al. Impact of hypertension on retinal capillary microvasculature using optical coherence tomographic angiography. *J Hypertens*. 2019;37:572–580.
62. Cringle SJ, Yu D-Y. A multi-layer model of retinal oxygen supply and consumption helps explain the muted rise in inner retinal Po2 during systemic hyperoxia. *Comp Biochem Physiol A Mol Integr Physiol*. 2002;132(1):61–66.
63. Wang S, Linsenmeier RA. Hyperoxia improves oxygen consumption in the detached feline retina. *Invest Ophthalmol Vis Sci*. 2007;48:1335–1341.
64. Palkovits S, Lasta M, Told R, et al. Retinal oxygen metabolism during normoxia and hyperoxia in healthy subjects. *Invest Ophthalmol Vis Sci*. 2014;55:4707–4713.
65. Wilson DF, Erecińska M. Effect of oxygen concentration on cellular metabolism. *Chest*. 1985;88:229S–232S.
66. Wang L, Kondo M, Bill A. Glucose metabolism in cat outer retina. Effects of light and hyperoxia. *Invest Ophthalmol Vis Sci*. 1997;38:48–55.

67. Natoli R, Fernando N, Dahlenburg T, et al. Obesity-induced metabolic disturbance drives oxidative stress and complement activation in the retinal environment. *Mol Vis*. 2018;24:201–217.
68. Liu X, He X, Yin Y, et al. Retinal oxygen saturation in 1461 healthy children aged 7–19 and its associated factors. *Acta Ophthalmol*. 2019;97(3):287–295.
69. Dai C, Liu X, Zhang HF, Puliafito CA, Jiao S. Absolute retinal blood flow measurement with a dual-beam Doppler optical coherence tomography. *Invest Ophthalmol Vis Sci*. 2013;54:7998–8003.
70. Garhofer G, Werkmeister R, Dragostinoff N, Schmetterer L. Retinal blood flow in healthy young subjects. *Invest Ophthalmol Vis Sci.* 2012;53:698–703.
71. Lee B, Novais EA, Waheed NK, et al. En face Doppler optical coherence tomography measurement of total retinal blood flow in diabetic retinopathy and diabetic macular edema. *JAMA Ophthalmol*. 2017;135:244–251.
72. Wang Y, Fawzi AA, Tan O, Zhang X, Huang D. Flicker-induced changes in retinal blood flow assessed by Doppler optical coherence tomography. *Biomed Opt Express*. 2011;2:1852–1860.
73. Srinivas S, Tan O, Wu S, et al. Measurement of retinal blood flow in normal Chinese-American subjects by Doppler Fourier-domain optical coherence tomography. *Invest Ophthalmol Vis Sci*. 2015;56:1569–1574.
74. Oishi A, Hidaka J, Yoshimura N. Quantification of the image obtained with a wide-field scanning ophthalmoscope. *Invest Ophthalmol Vis Sci*. 2014;55:2424–2431.
75. Jeppesen SK, Bek T. The retinal oxygen saturation measured by dual wavelength oximetry in larger retinal vessels is influenced by the linear velocity of the blood. *Curr Eye Res*. 2019;44:46–52.
76. Flammer J, Orgül S, Costa VP, et al. The impact of ocular blood flow in glaucoma. *Prog Retin Eye Res*. 2002;21:359–393.